

Chemical Science

rsc.li/chemical-science



ISSN 2041-6539



EDGE ARTICLE

Julius F. Kögel, Alexey Y. Timoshkin *et al.*
 $\text{Al}(\text{OCAr}^{\text{F}_3})_3$ – a thermally stable Lewis superacid



Cite this: *Chem. Sci.*, 2018, 9, 8178

All publication charges for this article have been paid for by the Royal Society of Chemistry

Received 6th July 2018
Accepted 25th September 2018

DOI: 10.1039/c8sc02981d

rsc.li/chemical-science

Al(OCAr^F)₃ – a thermally stable Lewis superacid†‡

Julius F. Kögel,^{a*} Alexey Y. Timoshkin,^{b*} Artem Schröder,^a Enno Lork^a and Jens Beckmann^a

The adduct free Lewis superacid Al(OCAr^F)₃ was obtained by the reaction of Ar^F₃COH with AlEt₃ and fully characterized (Ar^F = C₆F₅). It comprises a high thermal stability up to 180 °C and a distinct reactivity towards Lewis bases, as exemplified by the isolation of the neutral adducts Al(OCAr^F)₃·D (D = MeCN, THF, Et₂O, pyridine, OPEt₃), the fluoride complexes [Q][Al(OCAr^F)₃] (Q⁺ = Cs⁺, Ag⁺, Tl⁺, [S(NMe₂)₃]⁺, [Ph₃C]⁺, Li⁺, [NBu₄]⁺, [FeCp₂]⁺) and the chloride complex [Ph₃C][ClAl(OCAr^F)₃].

Introduction

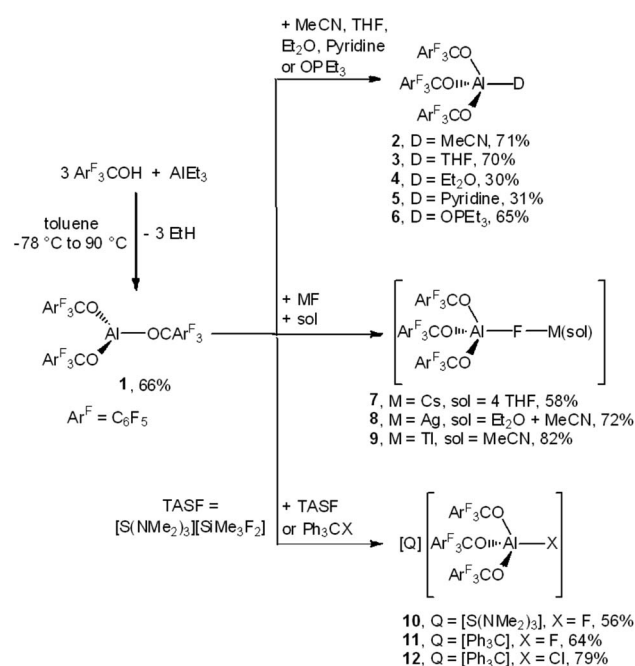
Lewis acids play a key role in many branches of chemistry. For instance, they are used as catalysts,¹ as components in frustrated Lewis pairs (FLPs)² and for the stabilization of unusual cations *via* formation of related weakly coordinating anions (WCAs).³ The strength of Lewis acids is usually estimated by the calculation of the fluoride ion affinity (FIA).^{4–8} The widely used B(C₆F₅)₃ (BCF) exhibits a FIA of 452 kJ mol⁻¹.⁸ Lewis superacids were defined as compounds exceeding the FIA of molecular SbF₅ (501 kJ mol⁻¹).⁹ Readily available aluminum halides, such as AlCl₃ and AlBr₃, are Lewis superacids in the gas phase, but exhibit a dramatically lower acidity in condensed phase due to dimerization. The key player in Lewis superacid chemistry is unarguably Krossing's Al(OC(CF₃)₃)₃ (FIA = 547 kJ mol⁻¹),⁹ which, however, has never been isolated.⁸ Due to its limited thermal stability it is usually prepared *in situ* and used as fluorobenzene adduct with a lower FIA (465 kJ mol⁻¹).⁹ Another drawback is the tendency of the corresponding WCAs, [Al(OC(CF₃)₃)₄]⁻ or [FAl(OC(CF₃)₃)₃]⁻, to suffer from severely disordered crystal structures.¹⁰ The vital interest in new Lewis superacids with more refined properties is highlighted by five recent publications: Mitzel *et al.* improved the Lewis acidity of BCF by substitution of its *para*-positions by CF₃ groups resulting in the strongest single-site triorganoborane Lewis acid B(C₆F₄CF₃)₃.¹¹ Riedel *et al.* reported on the isolation of the temperature sensitive superacid

Al(OTeF₅)₃ and its acetonitrile adduct together with a series of salts containing the new WCA [Al(OTeF₅)₄]⁻.¹² Sundermeyer and Krossing *et al.* described the extremely sensitive Lewis superacid Al(N(C₆F₅)₂)₃ with a high FIA of 555 kJ mol⁻¹.¹³ Only recently the group of Greb published a neutral silicon Lewis superacid¹⁴ and a review article on Lewis superacidity.¹⁵

Results and discussion

The free Lewis acid Al(OCAr^F)₃

We identified the perfluorinated alcohol Ar^F₃COH as a promising ligand for the preparation of new Lewis superacids (Ar^F = C₆F₅).¹⁶



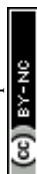
Scheme 1 Synthesis of Al(OCAr^F)₃ (1) and reactivity towards Lewis bases.

^aFB Biologie/Chemie, Universität Bremen, Leobener Str. 7, 28359 Bremen, Germany. E-mail: koegel@uni-bremen.de

^bInstitute of Chemistry, St. Petersburg State University, Universitetskaya emb. 7/9, 199034 St. Petersburg, Russia. E-mail: a.y.timoshkin@spbu.ru

† Ar^F = C₆F₅.

‡ Electronic supplementary information (ESI) available: Experimental procedures as well as computational and crystallographic details are reported in the electronic supplement. CCDC 1818681–1818687, 1863847–1863852 and 1866467. For ESI and crystallographic data in CIF or other electronic format see DOI: 10.1039/c8sc02981d



Indeed, the reaction of triethylaluminum with three equivalents of $\text{Al}^{\text{F}}\text{COH}$ provided the adduct free $\text{Al}(\text{OCAr}_3^{\text{F}})_3$ (**1**), which crystallized directly from the reaction mixture in 66% yield (Scheme 1). Unlike $\text{Al}(\text{OC}(\text{CF}_3)_3)_3$, **1** can be stored indefinitely under argon at room temperature. In fact, the thermal decomposition of **1** according to a DTA analysis occurs only above 180 °C. The molecular structure of $\text{Al}(\text{OCAr}_3^{\text{F}})_3$ (**1**) reveals that the spatial arrangement of the Al atoms is distorted trigonal bipyramidal and defined by a $\text{O}_3 + \text{F}_2$ donor set (Fig. 1): the three equatorial Al–O bonds (1.681(1)–1.701(1) Å) are significantly shorter than the two axial Al···F contacts (2.083(1) and 2.153(1) Å). These contacts, arising from intramolecular coordination of F atoms situated in the *ortho*-positions of two perfluorophenyl groups, are probably the reason for the increased thermal stability. A similar $\kappa\text{-O}_3\text{F}_2$ configuration was found in the molecular structure of $\text{Al}(\text{OC}(\text{C}_5\text{F}_{10})\text{C}_6\text{F}_5)_3$ (Al···F: 2.085(2) and 2.113(2) Å)⁷ and $\text{Al}(\text{N}(\text{C}_6\text{F}_5)_2)_3$ (Al···F: 2.060(1) and 2.084(1) Å)¹³ and calculated for adduct free $\text{Al}(\text{OC}(\text{CF}_3)_3)_3$ (Al···F: 2.143 and 2.155 Å).⁶

Theoretical section

The computed gas phase structure of **1** closely resembles the solid state structure, however, the computed bond distances (Al–O: 1.698, 1.711 and 1.719 Å; Al···F: 2.131 and 2.173 Å) are slightly longer. In order to evaluate the Lewis acidity, the FIA of **1** and related Lewis acids have been evaluated using *ab initio* MP2/6-311++G(2d,2p) single point energies at B3LYP/6-311++G(2d,2p) optimized geometries (Fig. 2). In addition to FIA computed using the reaction *via* direct F^- addition to LA, FIA values were also computed using the isodesmic reaction $\text{LA} + \text{COF}_2 = \text{LAF}^- + \text{COF}_2$ and the experimental gas phase FIA value of COF_2 (209 kJ mol⁻¹).⁵ For example, this approach was recently used by Stephan and coworkers.¹⁷ The differences between FIA values obtained from F^- addition reactions and from the isodesmic reactions are less than 4 kJ mol⁻¹

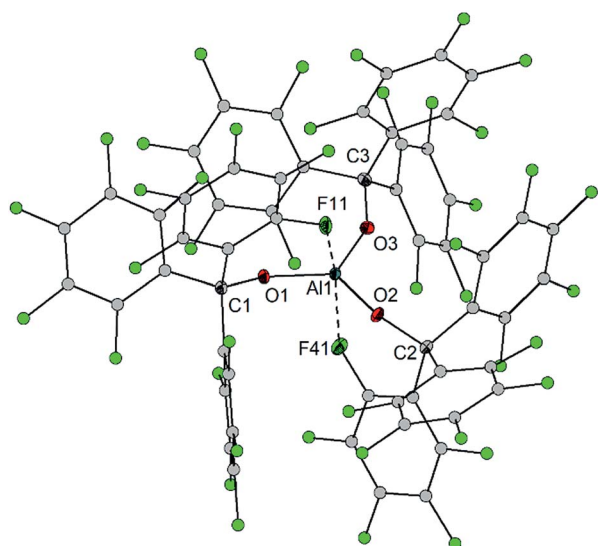


Fig. 1 Molecular structure of $\text{Al}(\text{OCAr}_3^{\text{F}})_3$ (**1**). Ellipsoids are set to 50% probability. Balls are drawn with an arbitrarily fixed radius.



Fig. 2 Fluoride ion affinities (FIAs) of selected Lewis acids ($\text{Ar}^{\text{F}} = \text{C}_6\text{F}_5$).

(Table S3[†]), indicating that the chosen approach allows to compute FIA *via* direct attachment of an F^- ion. The FIA values for the reference Lewis acids AlCl_3 , SbF_5 , BF_3 , $\text{B}(\text{C}_6\text{F}_5)_3$, and $\text{Al}(\text{OC}(\text{CF}_3)_3)_3$ computed in this work are close to the values reported in the literature at different levels of theory.⁸ The computed FIA values of $\text{Al}(\text{OC}(\text{CF}_3)_3)_3$ and **1** (Table S2[†]) are close, but taking into account the fact that $\text{Al}(\text{OC}(\text{CF}_3)_3)_3$ is isolable only as the fluorobenzene adduct $\text{Al}(\text{OC}(\text{CF}_3)_3)_3 \cdot \text{PhF}$, **1** is expected to be a stronger Lewis superacid by 90 kJ mol⁻¹ compared to the adduct.

Reactivity of $\text{Al}(\text{OCAr}_3^{\text{F}})_3$ towards Lewis bases

Having computationally established the high Lewis acidity of $\text{Al}(\text{OCAr}_3^{\text{F}})_3$ (**1**), we directed our attention to its reactivity towards Lewis bases. In non-coordinating solvents, such as toluene or dichloromethane, the solubility of **1** at room temperature is very poor. When a solution of **1** in toluene is treated with neutral Lewis bases, the adducts $\text{Al}(\text{OCAr}_3^{\text{F}})_3 \cdot \text{MeCN}$ (**2**), $\text{Al}(\text{OCAr}_3^{\text{F}})_3 \cdot \text{THF}$ (**3**), $\text{Al}(\text{OCAr}_3^{\text{F}})_3 \cdot \text{Et}_2\text{O}$ (**4**), $\text{Al}(\text{OCAr}_3^{\text{F}})_3 \cdot \text{pyridine}$ (**5**) and $\text{Al}(\text{OCAr}_3^{\text{F}})_3 \cdot \text{OPET}_3$ (**6**) were obtained (Scheme 1). The ¹H NMR chemical shifts (CD_2Cl_2) of the coordinating solvent molecules (*e.g.*: **2**: $\delta = 2.57$ ppm, **3**: $\delta = 3.88$ and 1.96 ppm) differ from those of the free solvents (MeCN : $\delta = 1.98$ ppm, THF : $\delta = 3.68$ and 1.82 ppm). The molecular structures of **2–6** show that the spatial arrangement of the Al atoms is distorted tetrahedral and defined by $\text{O}_3 + \text{N}$ and $\text{O}_3 + \text{O}$ donor sets, respectively (Fig. 3). Unlike **1**, the adducts show no intramolecular Al···F contacts. The primary Al–O bond distances of **2–6** closely resemble those of **1**. The molecular structure of **2** reveals an Al–N bond length of 1.941(1) Å and a C–N bond length of 1.134(2) Å which is shorter than in free acetonitrile (1.141(2) Å),¹⁸ which was also found for other Lewis acid base adducts ($\text{AlMe}_3 \cdot \text{MeCN}$: 1.136(3) Å,¹⁹ $\text{B}(\text{C}_6\text{F}_5)_3 \cdot \text{MeCN}$: 1.124(3) Å,¹⁸ $[\text{Cp}_3\text{Zr}(\text{MeCN})][\text{MeB}(\text{C}_6\text{F}_5)_3]$: 1.126(5) Å²⁰). The Al–O_{THF} bonds of **3** (1.866(2) and 1.872(2) Å) are slightly longer than that of $\text{Al}(\text{OC}(\text{CF}_3)_3)_3 \cdot \text{THF}$ (1.824(2) Å).²¹

The experimental Lewis acidity of $\text{Al}(\text{OCAr}_3^{\text{F}})_3$

The Lewis acidity of **1** was investigated experimentally by three different methods: (1) considering the C–N stretching vibration of **2**, (2) using the Gutmann–Beckett method and (3) in a competition experiment for fluoride ions with $[\text{SbF}_6]^-$.



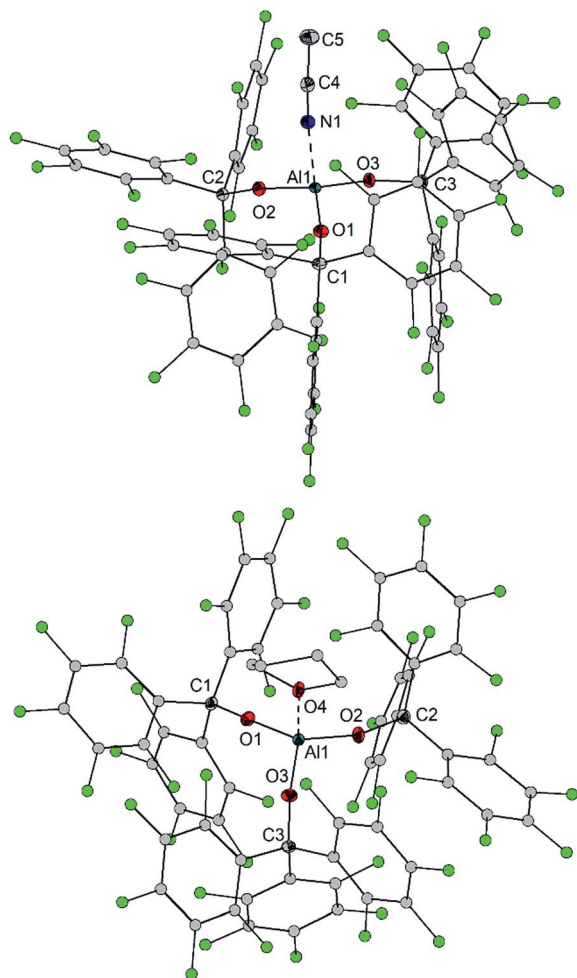


Fig. 3 Molecular structures of $\text{Al}(\text{OCArF}_3)_3 \cdot \text{MeCN}$ (**2**, top) and $\text{Al}(\text{OCArF}_3)_3 \cdot \text{THF}$ (**3**, bottom; ellipsoids with 50% probability, balls with an arbitrarily fixed radius; hydrogen atoms, non-coordinating solvent molecules and a second molecular moiety in the THF adduct omitted for clarity).

(1) The C–N stretching vibration of $\text{Al}(\text{OCArF}_3)_3 \cdot \text{MeCN}$. The C–N stretching vibration of **2** (2344 cm^{-1}) is blue-shifted compared to free acetonitrile (2253 cm^{-1});¹⁸ more blue-shifted than other Lewis acid MeCN adducts including $[\text{Cp}_3\text{Zr}(\text{MeCN})][\text{MeB}(\text{C}_6\text{F}_5)_3]$ (2321 cm^{-1}),²⁰ $\text{SbF}_5 \cdot \text{MeCN}$ (2335 cm^{-1}),²² and $\text{Al}(\text{OTeF}_5)_3 \cdot \text{MeCN}$ (2340 cm^{-1}),¹² which correlates with the higher acid strength of **1** compared to other parent Lewis acids. However, it should be noted that the CN stretching mode of the acetonitrile adduct of the considerably less Lewis acidic BCF exhibits an even higher value of 2367 cm^{-1} .¹⁸ The difficulty of the correlation of frequency of the C–N stretching mode with the Lewis acidity due to the Fermi coupling between $\nu(\text{CN})$ and $\nu(\text{CC}) + \delta_s(\text{CH}_3)$ was pointed out by Krahl and Kemnitz.²³ Hence, the adduct with deuterated acetonitrile was prepared also revealing a strong blueshift in the C–N stretching vibration ($\text{Al}(\text{OCArF}_3)_3 \cdot \text{CD}_3\text{CN}$: 2338 cm^{-1} , free CD_3CN : 2258 cm^{-1} ,¹² $\text{Al}(\text{OTeF}_5)_3 \cdot \text{CD}_3\text{CN}$: 2328 cm^{-1}).¹² Greb suggested to restrict the comparison of the C–N stretching modes to compounds of high similarity.¹⁵

(2) The Gutmann–Beckett method. The Gutmann–Beckett method uses the change of the ^{31}P NMR shift of OPEt_3 after coordination to a Lewis acidic center resulting in the so-called acceptor number (AN) as a benchmark for Lewis acidity.²⁴ $\text{Al}(\text{OCArF}_3)_3 \cdot \text{OPEt}_3$ exhibits a ^{31}P NMR shift of 73.9 ppm in CD_2Cl_2 corresponding to a low AN of 72.7 compared to Lewis acids with a lower FIA (e.g. $\text{B}(\text{C}_6\text{F}_5)_3$: 78.1 (CD_2Cl_2),²⁵ $\text{B}(\text{OC}_6\text{F}_5)_3$: 88.2 (C_6D_6),²⁶ $\text{BF}_3 \cdot \text{Et}_2\text{O}$: 84.0 (CDCl_3)).²⁷ However, the induced change of the ^{31}P NMR shift does not only depend on the Lewis acidity, but also on HSAB and sterical effects. The large $\text{OC}(\text{C}_6\text{F}_5)_3$ moieties provide sterical shielding of the aluminum center not allowing a small Al–O distance. Thus, the Gutmann–Beckett method seems unsuitable for the evaluation of the Lewis acidity of **1**.

(3) A competition experiment. As an experimental prove for Lewis superacidity, a competition experiment between **1** and $[\text{NBu}_4][\text{SbF}_6]$ was performed in toluene (Scheme 2). It revealed the formation of $[\text{FAl}(\text{OCArF}_3)_3]^-$ via ^{19}F NMR spectroscopy²⁸ suggesting a higher fluoride affinity of **1** compared to SbF_5 .

As discussed in the literature,¹⁵ method (1) and (2) gave ambiguous results concerning the Lewis acidity of **1** and seem unsuitable in this context. However, the competition experiment (3) is in agreement with the calculated trend of the fluoride ion affinity and proves the Lewis superacidity of **1**.

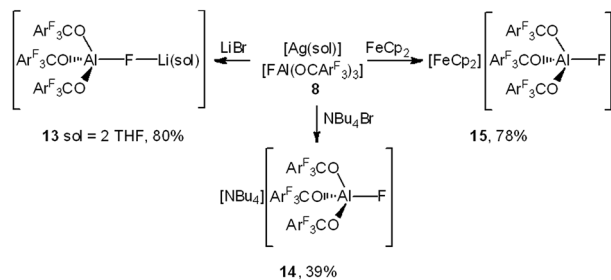
The weakly coordinating anions $[\text{FAl}(\text{OCArF}_3)_3]^-$ and $[\text{ClAl}(\text{OCArF}_3)_3]^-$

The utility of Lewis acids goes hand in hand with their ability to form metallates, which can act as weakly coordinating anions.²⁹ The reaction of **1** with several fluoride sources gave rise to a series of salts containing the WCA $[\text{FAl}(\text{OCArF}_3)_3]^-$ with different counteranions (Scheme 1, 7–11): The conversion of **1** with $[\text{S}(\text{NMe}_2)_3][\text{Me}_3\text{SiF}_2]$ in THF gave $[\text{S}(\text{NMe}_2)_3][\text{FAl}(\text{OCArF}_3)_3]$ (**10**). It revealed ^{19}F NMR chemical shifts of $\delta = -140.6, -159.6, -167.0$ and -178.4 ppm (CD_2Cl_2) with the aluminum bound fluorine atom exhibiting the strongest high-field shift ($[\text{Ag}(\text{Me}_2\text{SiO})_6][\text{FAl}(\text{OC}(\text{CF}_3)_3)_3]$: $\delta = -176.3$ ppm,³⁰ $[\text{Cs}(\text{ToI})_3][\text{FAl}(\text{N}(\text{C}_6\text{F}_5)_2)_3]$: $\delta = -157.4$ ppm).¹³ The trityl salt $[\text{Ph}_3\text{C}][\text{FAl}(\text{OCArF}_3)_3]$ (**11**) was prepared by the reaction of $\text{Al}(\text{OCArF}_3)_3$ (**1**) with Ph_3CF in toluene in 64% yield.¹³ An analogous procedure using Ph_3CCl gave the corresponding chloroaluminate $[\text{Ph}_3\text{C}][\text{ClAl}(\text{OCArF}_3)_3]$ (**12**) in 79% yield. Trityl salts of WCAs are frequently used as hydride or methyl group abstraction reagents, e.g. for the *in situ* generation of metallocene cations for the catalytic polymerization of alkenes³¹ and are also used as mild one-electron oxidants.³² The metal salts $[\text{M}(\text{sol})][\text{FAl}(\text{OC}(\text{CF}_3)_3)_3]$ ($\text{M} = \text{Cs}, \text{Ag}, \text{Tl}$; sol = THF, Et_2O , MeCN) were obtained from reacting **1** with CsF, AgF and TlF in acetonitrile. The silver and thallium salts of the WCA have the



Scheme 2 Abstraction of a fluoride ion from SbF_6^- by $\text{Al}(\text{OCArF}_3)_3$.





Scheme 3 Reaction of the silver salt **8** with LiBr, NBU₄Br and ferrocene.

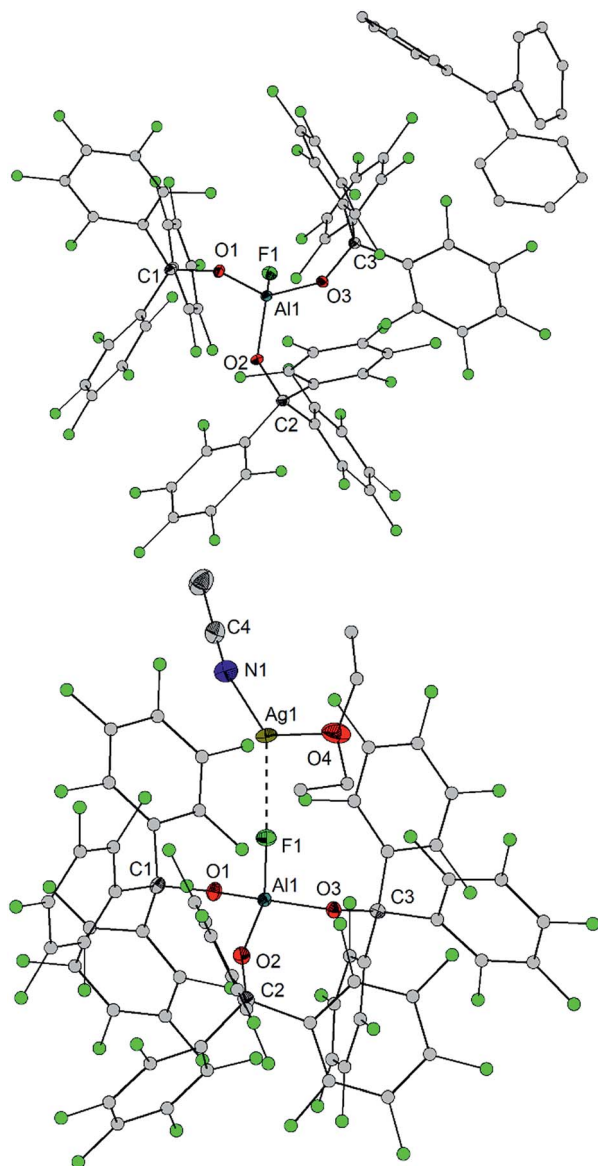


Fig. 4 Molecular structure of $[\text{Ph}_3\text{C}][\text{FAl}(\text{OCAr}^{\text{F}_3})_3]$ (Al1–F1 1.683(1) Å) (left) and $[\text{Ag}(\text{MeCN})(\text{Et}_2\text{O})][\text{FAl}(\text{OCAr}^{\text{F}_3})_3]$ (Al1–F1 1.698(1) Å, F1...Ag1 2.310(1) Å, F1...Ag1a 2.224(4) Å) (right) (ellipsoids with 50% probability, balls with a arbitrarily fixed radius; hydrogen atoms and non-coordinating solvent molecules omitted for clarity; a positional disorder found for the Ag atom with an occupancy ratio of 0.85 : 0.15 is not displayed).

potential to generate reactive cations by halide ion abstraction, whereby the driving force is the precipitation of sparingly soluble silver or thallium halides. Silver salts of WCAs serve also as mild oxidants (Scheme 3). The use of the silver salt **8** was demonstrated in the reactions with lithium bromide and tetrabutyl ammonium bromide in which the precipitation of silver bromide gave rise to $[\text{Li}(\text{THF})_2][\text{FAl}(\text{OCAr}^{\text{F}_3})_3]$ **13** and $[\text{NBU}_4][\text{FAl}(\text{OCAr}^{\text{F}_3})_3]$ **14**, respectively (Scheme 3). **13** is suitable for salt metathesis reactions. Furthermore, **8** is able to oxidize ferrocene in dichloromethane to the ferrocenium salt $[\text{FeCp}_2][\text{FAl}(\text{OCAr}^{\text{F}_3})_3]$ (**15**) which could act as a milder oxidant.

The aluminates **7–9** and **11–15** were structurally characterized by X-ray crystallography (Fig. 4 and S5–S10[†]). Like in the neutral Lewis acid base adducts **2–6**, the spatial arrangement of **7–9** and **11–15** is tetrahedral. The Al–O distances found in the anions $[\text{FAl}(\text{OCAr}^{\text{F}_3})_3]^-$ (e.g. 1.726(1), 1.745(1) and 1.745(1) Å in **11**) are slightly elongated compared to the free Lewis acid **1** (1.681(1)–1.701(1) Å). The Al–F distances range from 1.678(1) Å in $[\text{NBU}_4][\text{FAl}(\text{OCAr}^{\text{F}_3})_3]$ to 1.759(2) Å in $[\text{Li}(\text{Et}_2\text{O})_2][\text{FAl}(\text{OCAr}^{\text{F}_3})_3]$ being considerably shorter than the hemilabile Al...F contacts of the free Lewis acid **1** (2.083(1) and 2.153(1) Å). In **7–9** and **13**, there are weak cation...anion contacts between the metal ions and the Al–F (Cs...F: 2.886(2) and 2.869(2) Å, Ag...F: 2.314(1) and 2.224(4) Å, Tl...F: 2.506(2) Å, Li...F: 1.828(6) Å), which are absent in the $[\text{Ph}_3\text{C}]^+$, $[\text{S}(\text{NMe}_2)_3]^+$, $[\text{NBU}_4]^+$ and $[\text{FeCp}_2]^+$ salts. The latter compounds tend to exhibit slightly shorter Al–F bond lengths. In the calculated $[\text{FAl}(\text{OCAr}^{\text{F}_3})_3]^-$ anion, the Al–O distances (1.756 Å) and the Al–F distance (1.699 Å) are somewhat longer than the experimental values,³³ but comparable to the Al–F distances found for $[\text{Ag}(\text{Me}_2\text{SiO})_6][\text{FAl}(\text{OC}(\text{CF}_3)_3)_3]$ (1.677(4) Å)³⁰

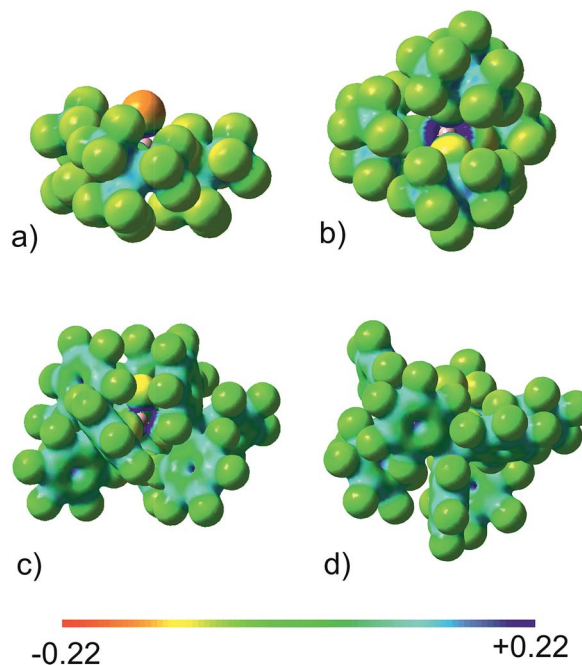


Fig. 5 Projection of the calculated electrostatic potential on the 0.025 e[−] bohr^{−3} isodensity surface. (a) $[\text{FAl}(\text{OC}(\text{CF}_3)_3)_3]^-$; (b) $[\text{Al}(\text{OC}(\text{CF}_3)_3)_4]^-$; (c) $[\text{FAl}(\text{OCAr}^{\text{F}_3})_3]^-$; (d) $[\text{Al}(\text{OCAr}^{\text{F}_3})_3]^-$. B3LYP/6-311++G(2d,2p) level of theory.



and $[\text{Cs}(\text{Tol})_3][\text{FAl}(\text{N}(\text{C}_6\text{F}_5)_2)_3]$ (1.689(2) Å).¹³ The Al–Cl distance in $[\text{Ph}_3\text{C}][\text{ClAl}(\text{OCAr}_3^{\text{F}})_3]$ is 2.1748(6) Å.

The stability of $[\text{FAl}(\text{OCAr}_3^{\text{F}})_3]^-$ towards oxidation was investigated by cyclic voltammetry in acetonitrile revealing no oxidative processes at potentials of up to 2.2 V (vs. Fc/Fc^+). In order to evaluate the coordination ability of the WCAs, the electrostatic potential was calculated (Fig. 5). In contrast to $[\text{FAl}(\text{OC}(\text{CF}_3)_3)_3]^-$ (Fig. 5a) where the F atom bound to Al carries considerable negative charge and is quite open for the attack of the electrophile due to a lack of protection by $\text{OC}(\text{CF}_3)_3$ groups, the corresponding fluorine atom in $[\text{FAl}(\text{OCAr}_3^{\text{F}})_3]^-$ (Fig. 5c) and chlorine atom in $[\text{ClAl}(\text{OCAr}_3^{\text{F}})_3]^-$ (Fig. 5d) carry smaller charges and are shielded by the bulky $\text{OC}(\text{C}_6\text{F}_5)_3$ groups. Their electrostatic potentials resemble that of Krossing's classical WCA $[\text{Al}(\text{OC}(\text{CF}_3)_3)_4]^-$ (Fig. 5b).

In summary, the presented WCA salts can be utilized in broad range of applications: as oxidants (8, 11, 12, 15), in salt metathesis reactions (7–9, 13), in hydride or alkyl elimination reactions (11 and 12) or as supporting electrolytes (14) according to the scheme presented in ref. 29d.

Conclusions

Synthetic protocols for the synthesis of the new Lewis superacid $\text{Al}(\text{OCAr}_3^{\text{F}})_3$ (1), and its corresponding WCAs $[\text{FAl}(\text{OCAr}_3^{\text{F}})_3]^-$ and $[\text{ClAl}(\text{OCAr}_3^{\text{F}})_3]^-$ were developed. Compared to literature known Lewis superacids, 1 stands out due to its high FIA. Its high thermal stability allows the adduct free isolation as crystalline solid and storage under argon at room temperature. Furthermore, the WCAs $[\text{FAl}(\text{OCAr}_3^{\text{F}})_3]^-$ and $[\text{ClAl}(\text{OCAr}_3^{\text{F}})_3]^-$ show favorable crystallization behavior due to the absence of disorder and we present a versatile series of their salts with different counteranions as a toolbox for potential users. We hope these beneficial properties will encourage chemists from different fields to make use of these easily accessible compounds.

Conflicts of interest

There are no conflicts to declare.

Acknowledgements

We thank Prof. Dr Jörg Sundermeyer and Sebastian Ullrich for providing access to IR spectroscopic measurements under inert conditions. We thank Sarah Gansemer and Prof. Dr Anne Staubitz for TGA measurements and Daniel Duvinage and Dr Marian Olaru for support with the NMR spectroscopic measurements and cyclic voltammetry (D. D.) We thank Artem Zavgorodnii for his synthetic contribution. A. Y. T is grateful to RSF grant 18-13-00196.

Notes and references

- (a) A. Corma and H. Garcia, *Chem. Rev.*, 2003, **103**, 4307; (b) S. Kobayashi and K. Manabe, *Pure Appl. Chem.*, 2000, **72**, 1373; (c) F. Fringuelli, O. Piermatti, F. Pizzo and

- L. Vaccaro, *Eur. J. Org. Chem.*, 2001, 439; (d) J. Faller and J. Jonathan, *Curr. Org. Chem.*, 2006, **10**, 151.
- (a) C. Welch, R. R. San Juan, J. D. Masuda and D. W. Stephan, *Science*, 2006, **314**, 1124; (b) G. C. Welch, L. Cabrera, P. A. Chase, E. Hollink, J. D. Masuda, P. Wei and D. W. Stephan, *Dalton Trans.*, 2007, 3407. For recent reviews see (c) D. W. Stephan, *J. Am. Chem. Soc.*, 2015, **137**, 10018; (d) D. W. Stephan and G. Erker, *Angew. Chem.*, 2015, **127**, 6498; *Angew. Chem. Int. Ed.*, 2015, **54**, 6400.
- T. A. Engesser, M. R. Lichtenthaler, M. Schleep and I. Krossing, *Chem. Soc. Rev.*, 2016, **45**, 789.
- T. E. Mallouk, G. L. Rosenthal, G. Mueller, R. Brusasco and N. Bartlett, *Inorg. Chem.*, 1984, **23**, 3167.
- K. O. Christe, D. A. Dixon, D. McLemore, W. W. Wilson, J. Sheehy and J. A. Bootz, *J. Fluorine Chem.*, 2000, **101**, 151.
- L. O. Müller, D. Himmel, J. Stauffer, G. Steinfeld, J. Slattery, G. Santiso-Quiñones, V. Brecht and I. Krossing, *Angew. Chem.*, 2008, **120**, 7772; *Angew. Chem. Int. Ed.*, 2008, **47**, 7659.
- A. Kraft, N. Trapp, D. Himmel, H. Böhrer, P. Schlüter, H. Scherer and I. Krossing, *Chem.–Eur. J.*, 2012, **18**, 9371.
- H. Böhrer, N. Trapp, D. Himmel, M. Schleep and I. Krossing, *Dalton Trans.*, 2015, **44**, 7489.
- Calculated within this work (*vide infra*).
- For examples see: (a) A. Reisinger, N. Trapp, I. Krossing, S. Altmannshofer, V. Herz, M. Presnitz and W. Scherer, *Angew. Chem.*, 2007, **119**, 8445; *Angew. Chem. Int. Ed.*, 2007, **46**, 8295; (b) I. Raabe, C. Röhr and I. Krossing, *Dalton Trans.*, 2007, **36**, 5376; (c) D. Aris, J. Beck, A. Decken, I. Dionne, J. Schmedt auf der Günne, W. Hoffbauer, T. Köchner, I. Krossing, J. Passmore, E. Rivard, F. Steden and X. Wang, *Dalton Trans.*, 2011, **40**, 5865; (d) H. Poleschner and K. Seppelt, *Angew. Chem.*, 2013, **125**, 13072; *Angew. Chem. Int. Ed.*, 2013, **52**, 12838.
- L. A. Körte, J. Schwabedissen, M. Soffner, S. Blomeyer, C. G. Reuter, Y. V. Vishnevskiy, B. Neumann, H.-G. Stammler and N. W. Mitzel, *Angew. Chem.*, 2017, **129**, 8701; *Angew. Chem. Int. Ed.*, 2017, **56**, 8578.
- (a) A. Wiesner, T. W. Gries, S. Steinhauer, H. Beckers and S. Riedel, *Angew. Chem.*, 2017, **129**, 8375; *Angew. Chem. Int. Ed.*, 2017, **56**, 8263; (b) K. F. Hoffmann, A. Wiesner, N. Subat, S. Steinhauer and S. Riedel, *Z. Anorg. Allg. Chem.*, 2018, DOI: 10.1002/zaac.201800174.
- J. F. Kögel, D. A. Sorokin, A. Khvorost, M. Scott, K. Harms, D. Himmel, I. Krossing and J. Sundermeyer, *Chem. Sci.*, 2018, **9**, 245.
- R. Maskey, M. Schädler, C. Legler and L. Greb, *Angew. Chem.*, 2018, **130**, 1733; *Angew. Chem. Int. Ed.*, 2018, **57**, 1717 Also see: A. L. Liberman-Martin, R. G. Bergman and T. D. Tilley, *J. Am. Chem. Soc.*, 2015, **137**, 5328.
- L. Greb, *Chem.–Eur. J.*, 2018, DOI: 10.1002/chem.201802698.
- (a) R. D. Chambers and D. J. Spring, *J. Chem. Soc. C*, 1968, 2394; (b) S. V. Kulkarni, R. Schure and R. Filler, *J. Am. Chem. Soc.*, 1973, **95**, 1859.
- R. Jupp, T. C. Johnstone and D. W. Stephan, *Dalton Trans.*, 2018, **47**, 7029.
- H. Jacobsen, H. Berke, S. Döring, G. Kehr, G. Erker, R. Fröhlich and O. Meyer, *Organometallics*, 1999, **18**, 1724.



- 19 M. R. Kopp and B. Neumüller, *Z. Anorg. Allg. Chem.*, 1999, **625**, 739.
- 20 T. Brackemeyer, G. Erker, R. Fröhlich, J. Prigge and U. Peuchert, *Chem. Ber./Recl.*, 1997, **130**, 899.
- 21 B. von Ahsen, B. Bley, S. Proemmel, R. Wartchow, H. Willner and F. Aubke, *Z. Anorg. Allg. Chem.*, 1998, **624**, 1225.
- 22 T. Krahl and E. Kemnitz, *J. Fluorine Chem.*, 2006, **127**, 663–678.
- 23 A. Bihlmeier, M. Gonsior, I. Raabe, N. Trapp and I. Krossing, *Chem.–Eur. J.*, 2004, **10**, 5041.
- 24 (a) U. Mayer, V. Gutmann and W. Gerger, *Monatsh. Chem.*, 1975, **106**, 1235; (b) M. A. Beckett, G. C. Strickland, J. R. Holland and K. S. Varma, *Polymer*, 1996, **37**, 4629.
- 25 A. E. Ashley, T. J. Herrington, G. G. Wildgoose, H. Zaher, A. L. Thompson, N. H. Rees, T. Krämer and D. O'Hare, *J. Am. Chem. Soc.*, 2011, **133**, 14727.
- 26 G. J. P. Britovsek, J. Ugoletti and A. J. P. White, *Organometallics*, 2005, **24**, 1685.
- 27 E. L. Myers, C. P. Butts and V. K. Aggarwal, *Chem. Commun.*, 2006, 4434.
- 28 Also the formation of free $(C_6F_5)_3COH$ was detected as a consequence of the formation of HF from the reaction between SbF_5 and toluene. G. A. Olah, P. Schilling and I. M. Gross, *J. Am. Chem. Soc.*, 1974, **96**, 876.
- 29 (a) S. H. Strauss, *Chem. Rev.*, 1993, **93**, 927; (b) I. Krossing and A. Reisinger, *Coord. Chem. Rev.*, 2006, **250**, 2721; (c) A. B. A. Rupp and I. Krossing, *Acc. Chem. Res.*, 2015, **48**, 2537; (d) I. M. Riddlestone, A. Kraft, J. Schaefer and I. Krossing, *Angew. Chem.*, 2018, DOI: 10.1002/ange.201710782; *Angew. Chem. Int. Ed.*, DOI: 10.1002/anie.201710782.
- 30 T. S. Cameron, A. Decken, I. Krossing, J. Passmore, J. M. Rautiainen, X. Wang and X. Zeng, *Inorg. Chem.*, 2013, **52**, 3113.
- 31 D. S. McGuinness, A. J. Rucklidge, R. P. Tooze and A. M. Z. Slawin, *Organometallics*, 2007, **26**, 2561.
- 32 E. F. van der Eide, W. E. Piers, M. Parvez and R. McDonald, *Inorg. Chem.*, 2007, **46**, 14.
- 33 B3LYP/6-311++G(2d,2p) level of theory (see ESI† for details).

